Research Article

Ahmed Aouissi*, Dhaifallah Aldhayan, Naaser A. Y. Abduh, and Abdullah Al Kahtani

Propylene carbonate synthesis from propylene oxide and CO$_2$ over Ga-Silicate-1 catalyst

Abstract: Gallosilicate zeolite (Ga-Silicate-1) was synthesized and characterized by wet chemical analysis, Fourier transform infrared spectroscopy, X-ray diffraction, BET surface area analysis and ^{29}Si MAS NMR. The prepared Ga-Silicate-1, calcined in the temperature range from 350°C to 550°C, was tested as a catalyst for the synthesis of propylene carbonate (PC) from CO$_2$ and propylene oxide in a solvent-free reaction. The effects of various parameters, such as co-catalyst, reaction temperature, reaction time, and pressure of CO$_2$, on the reaction were investigated. It has been found that increasing the calcination temperature from 500°C to 550°C decreased both the conversion and selectivity to PC from 63.7% to 20.6% and from 77.6% to 58.9%, respectively. Unlike conversion and selectivity, the surface area increased from 96.1 to 103.8 m^2/g. This significant increase in surface area due to the degalliation of the zeolite, along with the decrease in conversion, clearly indicates the role of gallium in the production of PC. Under mild reaction conditions (75°C and $P_{(CO_2)}$ = 0.55 MPa), a conversion of 70.8% and a selectivity of 81.3% were obtained. Based on the obtained results, a mechanism for the synthesis of PC over the Ga-Silicate-1 catalyst was proposed.

Keywords: carbon dioxide, cyclic carbonate, propylene oxide, gallosilicate, zeolite

* **Corresponding author: Ahmed Aouissi,** Department of Chemistry, King Saud University, P.O. Box 2455, Riyadh, 11451, Saudi Arabia, e-mail: aouissed@yahoo.fr, tel: +966 1 4675958, fax: +966 1 4675992
Dhaifallah Aldhayan, Naaser A. Y. Abduh, Abdullah Al Kahtani: Department of Chemistry, King Saud University, P.O. Box 2455, Riyadh, 11451, Saudi Arabia

1 Introduction

In the context of environmental protection and carbon economy, efforts have intensified in recent years to produce useful products by reacting carbon dioxide with chemicals. Among these reactions, that which leads to cyclic carbonates by the reaction of CO$_2$ with epoxides is of great industrial importance. In fact, cyclic carbonates are used in the synthesis of many chemicals and pharmaceuticals, in lithium-ion batteries, as electrolytic solvents, and as monomers in the thermoplastic industry [1–3]. Many homogeneous catalysts such as alkali metal salts [4], phosphonium/quaternary ammonium salts [5], bromine [6], ionic liquids [7], metal complexes [8–10], polyoxometalates [11], and organocatalysts [12] were used to catalyze this reaction. Unfortunately, homogeneous catalysts face the problem of recyclability. To avoid this drawback, heterogeneous catalytic systems have been developed, in particular metallic oxides [13,14], activated carbons doped with N in batch mode [15], organic metallic frameworks [16,17], and microspheres with an inorganic–organic hybrid shell [18]. Although heterogeneous catalysts have the advantage of being recyclable, they still have certain drawbacks such as the need for a large amount of catalyst, a long reaction time, or a very high carbon dioxide pressure. So, developing an efficient heterogeneous catalyst that can capture and convert CO$_2$ to cyclic carbonates under mild conditions is still a challenge.

Zeolites are mesoporous solids with a high specific surface area and an adjustable pore volume, making them capable of absorbing large quantities of CO$_2$ [18–20]. It has been reported that zeolites containing various metals show remarkable catalytic performance in the conversion of CO$_2$ [21,22]. Various zeolites modified by metals (MHZSM-5) were tested for the cycloaddition of CO$_2$ with propylene oxide (PO) [23]. It was found that the reaction was not catalyzed when only NaZSM-5 or HZSM-5 was used. On the other hand, when tetra-n-propylammonium bromide was used, propylene carbonate (PC) was obtained but with a low yield.

Surprisingly, when HZSM-5 is used in the presence of tetra-n-propylammonium bromide as the co-catalyst, the yield of PC increased to 70%. By using Fe(III), Co(II) and Ni(II) in place of Zn(II), the yields obtained decreased to 35%, 53%, and 33%, respectively. Another study on the cycloaddition of CO$_2$ to PO was carried out on a mesoporous titanium-silicalite zeolite as the catalyst. The zeolite that was prepared using polydiallyldimethylammonium chloride as the mesopore template was treated with hydrochloric acid aqueous solution and was not calcined [24]. The resulting organic–inorganic composite contains two active sites, basic sites from the organic template and acid sites coming from the framework Ti. The conversion of PO obtained under 1.6 MPa at 120°C for 6 h when acetonitrile is used as a solvent reached 80.1%, and the selectivity for PC was 97.8%. To the best of our knowledge, gallium-modified zeolites have not been used in the reaction of CO$_2$ with epoxides. Ga-modified zeolites were used for methanol conversion, alkylation, isomerization, and disproportionation of aromatics [25]. It is worth noting that the aromatization of alkanes into aromatic components on ZSM-5 modified Ga catalysts is commercialized in the Cyclar process developed by UOP and BP [26].

Several research studies have revealed that zeolites containing gallium are active catalysts [27–29], and it has been mentioned that a small amount of gallium can significantly increase the catalytic activity of ZSM-5 zeolites due to the synergistic effect of the properties of Ga$_2$O$_3$ and ZSM-5 [27,28]. These characteristics prompted us to study the catalytic activity of Ga-ZSM-5 for the cycloaddition of CO$_2$ to PO. The experiments were carried out under mild conditions and without solvent.

2 Materials and methods

2.1 Materials

All the chemicals used for the synthesis were used without further purification. PO and tetraethylammonium bromide (TEABr) (>99%) were purchased from Merck-Schuchardt (Hohenbrunn, Germany). Sodium silicate (29.25% wt SiO$_2$, 8.85% wt Na$_2$O, 61.9% wt H$_2$O) (Crossfield Chemicals), sodium aluminate NaAlO$_2$ (52.3% wt Al$_2$O$_3$, 47.7% wt Na$_2$O) (BDH Chemicals), and tetra propyl ammonium hydroxide TPAOH (20% aqueous solution) (Aldrich Chemicals Co.) were used.

2.2 Preparation of the catalyst – gallosilicate zeolite (Ga-Silicate-1)

A solution (A) was prepared by dissolving 3.62 g of gallium nitrate (Ga(NO$_3$)$_3$, 6H$_2$O) in distilled water (10.00 g), and sodium hydroxide (3.40 g) dissolved in 20.00 g of distilled water was added to solution (A) with stirring. Subsequently, 12.20 g of tetra-n-propyl ammonium bromide was added to the resulting solution. A second solution (B) was formed by mixing colloidal silica (45.00 g) with distilled water (20.00 g). Solution (B) was then added dropwise to solution (A). After agitation for several minutes (approximately 20 min), the mixture was placed in an autoclave (100.00 mL capacity) and heated at 175°C under autogenous pressure for 3 days.

After the crystallization was complete, the products were filtered, washed with distilled water, and then dried overnight at 120°C. Thermal decomposition of the organic quaternary amine, still associated with the as-synthesized zeolite structure, was performed in flowing air at 540°C for 16 h.

2.3 Characterization of the catalysts

Infrared spectra were recorded with an infrared spectrometer, GENESIS II-FTIR (4,000–400 cm^{-1}), using the KBr pellet technique. X-ray diffraction (XRD) measurements were carried out employing an Ultima IV X-ray Rigaku diffractometer using Cu-Kα radiation. The specific surface area (BET), pore volume, and average pore diameter of the fresh and used catalysts were measured using a Micromeritics Tristar II 3020 surface area and porosity analyzer. To achieve these measurements, catalysts of weights varying from 0.200 to 0.500 g were used. Elemental composition analysis of samples was carried out by the Chemistry Department Microanalytical Services, UMIST, using standard (wet chemical) methods, involving the digestion of the sample into solution followed by analysis using atomic absorption. ^{29}Si Magic Angle Spinning Nuclear Magnetic Resonance Spectroscopy (^{29}Si MAS NMR) spectra of Ga-Silicate-1 samples were obtained by using a Jeol GNM GX 400 FTNMR spectrometer. Approximately 0.3 g of Ga-Silicate-1 was spun at the magic angle 54°44′ to the applied magnetic field at 4 KHz. Chemical shifts were recorded with respect to trimethylsilane for ^{29}Si as an external reference.

2.4 Procedure for the synthesis of PC

The reaction of PO and CO_2 was performed in an $80\,cm^3$ stainless steel autoclave equipped with a magnetic stirrer. In a typical run, the reaction mixture, PO, catalyst, and co-catalyst (TEABr) were charged into the autoclave and then purged with CO_2. The reaction mixture was then heated to the reaction temperature and pressurized with CO_2 to a preset pressure under stirring. The temperature of the autoclave is regulated using a circulating water bath. When the desired time elapsed, the reactor was cooled using the circulating water bath to 10°C and depressurized to atmospheric pressure. After slowly releasing the remaining CO_2, the products were separated from the reactant mixture by centrifugation and then analyzed with a gas phase chromatograph (PYE UNICAM) equipped with a flame ionization detector using a capillary column (HP-PLOT Q, length 30 m, ID 0.53 mm).

3 Results and discussion

3.1 Catalyst characterization

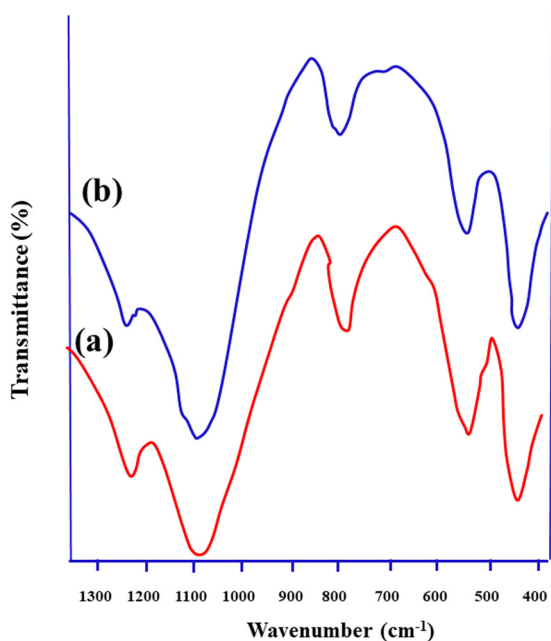In order to obtain the structural information of the synthesized Ga-silicate catalyst, samples of the as-synthesized and calcined Ga-silicate were characterized by IR, XRD, and ^{29}Si MAS NMR. For the purpose of zeolite framework characterization, attention is usually focused on the mid-infrared region (1,300 to $400\,cm^{-1}$) because this region contains the fundamental vibrations of SiO_4 or in general TO_4 units in all zeolite frameworks [25,30]. Figure 1 shows the infrared spectra of both samples. The MFI structure formation was confirmed by the bands near $432\,cm^{-1}$ (T–O bending vibration of the TO_4 internal tetrahedra), $547\,cm^{-1}$ (double ring vibration), $799\,cm^{-1}$ (external symmetric stretch), and $1,087\,cm^{-1}$, assigned to the internal asymmetric stretching of the T–O–T bond of the framework [24,26,31–33]. The band at $1,229\,cm^{-1}$, which is known as a structure-sensitive IR band of ZSM-5 zeolite, has been assigned to external linkages to TO_4 tetrahedra [33].

The X-ray powder diffraction patterns of both the as-synthesized and calcined Ga-silicate are shown in Figure 2. Both samples show the peaks corresponding to

Figure 1: FTIR spectra of (a) as-synthesized Ga-Silicate-1 and (b) Ga-Silicate-1 calcined at 550°C for 16 h.
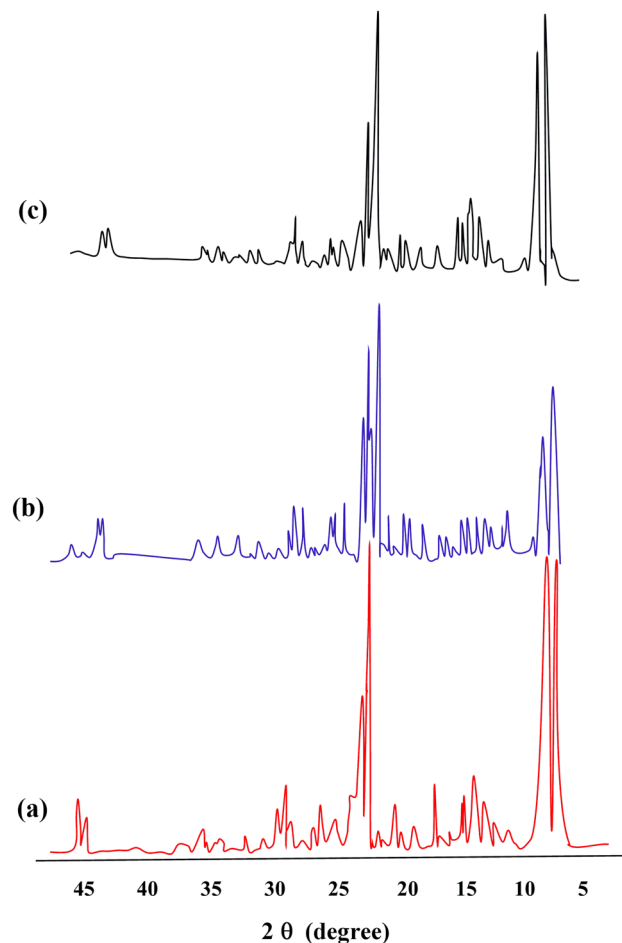

Figure 2: XRD of (a) Silicalite-1, (b) Ga-Silicate-1 "as-synthesized," and (c) Ga-Silicate-1 "calcined."

the MFI-type zeolite phase [34–36]. There were no observable XRD lines that correspond to any crystalline gallium oxides. When the sample was calcined, the relative intensity of the first two lines at 7.9° and 8.8° (2θ) increased greatly, whereas the lines at 11.9° and 12.5° (2θ) and the central peaks between 2θ of 22 and 24 reduced marginally. The doublet at about 14.6° (2θ) merged to form an apparent single line. There is appearance of doublets in place of singles (the peak at about 23.17° (2θ)). Compared to silicalite-1, Ga-silicate (Table 1) shows a shift toward higher d-spacing values and to lower angle regions. This is in agreement with the fact that when an element with the M–O bond longer than that of Si–O is inserted into the zeolite framework, the d-spacing frequently shifts toward higher d-spacing values. The observed lattice expansion may be a consequence of the incorporation of gallium ions into the silicate framework during the synthesis [37]. This result is corroborated by those reported in the literature [38,39], where it has been found that the diffraction peaks between 22.5° and 25° shifted to the lower angle region after the incorporation of Zn. In the opinion of the authors, this was due to the isomorphous substitution of tetrahedral Si atoms with Zn atoms possessing a larger radius and a longer Zn–O bond (1.95 Å) than the Si–O bond (1.62 Å). This result was also corroborated by other research studies reported in the literature, where an increase in the unit cell volumes in the presence of gallium has been observed. In the opinion of the authors, the result should be an indication of the probable incorporation of gallium in the MFI structure [40].

High-resolution ^{29}Si solid state Magic Angle Spinning NMR spectroscopy (^{29}Si MAS NMR) can distinguish between lattice silicon and aluminum and also provide information on structural units and heterogeneities. When a solid sample is spun at the magic angle to the magnetic field, chemical shifts can be easily identified. Based on the fact that the chemical shift values are characteristics of chemically and crystallographically distinct environments, two non-calcined samples of Ga-Silicate-1 with different Si/Ga ratios were examined. The results are illustrated in Figure 3. The Ga-Silicate-1 spectrum shows two peaks. The first one at –112 ppm is due to the Si linked in the framework by oxygen bridges to four silicon T-atoms, Si(OSi)₄ (i.e., Si(OGa)) units in the lattice, whereas the second one at –102 ppm can be assigned to a silicon atom with 3Si and Ga atoms in the second coordination sphere (Si(OSi)₃(OGa)). This result is in agreement with those reported in the literature. In fact, Khodakov et al. [41] attributed the signal at –105.3 ppm in the ^{29}Si MAS NMR of a Ga-Silicate-1 sample to the presence of gallium in a tetrahedral framework position [Si(1Ga)]. Jacob et al. [42] also attributed the signal at –104 ppm in the ^{29}Si MAS NMR of a gallium Nu-23 zeolite to Si(1Ga). Xin et al. [43] assigned the signals at –115 and –106 ppm to Q^4(4Si, 0 M) sites and Q^3(3Si, 1 M) sites (M = Al and/or Ga) in the framework structure, respectively. As the gallium content in the Ga-Silicate-1 samples is increased from 65.5 (Figure 4b) to 34.7 (Figure 4a), the signal at –112 ppm becomes broader, increasing the width from 6.0 to 9.7 ppm, and the shoulder that has been assigned to Si(1Ga) becomes more obvious. The broadening of the ^{29}Si MAS NMR signal of Ga-Silicate-1, resulting from the increase in the gallium content in the sample, is further evidence of the substitution of Ga(III) in the framework of the zeolite Ga-Silicate-1. A similar observation has been reported for zeolite Fe-ZSM-5 [44] and for Ga-ZSM-5 [43].
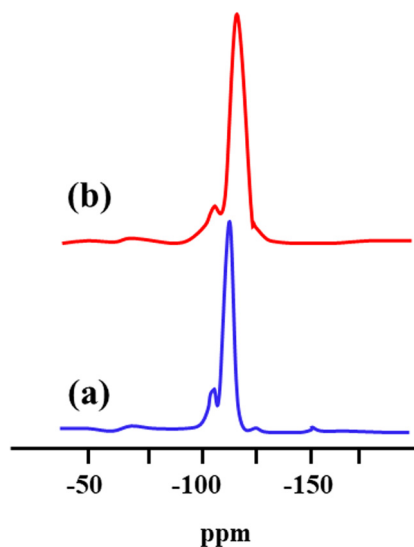
Table 1: Angle region and d-spacing for the main peaks of Silicalite-1 and Ga-silicate

Silicalite-1		Ga-silicate	
2θ (°)	d-spacing (Å)	2θ (°)	d-spacing (Å)
7.97	11.09	7.96	11.10
8.90	9.92	8.85	9.98
23.33	3.81	23.31	3.81
23.9	3.72	23.78	3.74
24.33	3.63	23.96	3.71
24.59	3.61	24.45	3.64

Figure 3: ^{29}Si NMA SNMR spectra of (a) Ga-Silicate-1 (Si/Ga 65.5) and (b) Ga-Silicate-1 (Si/Ga 34.7).
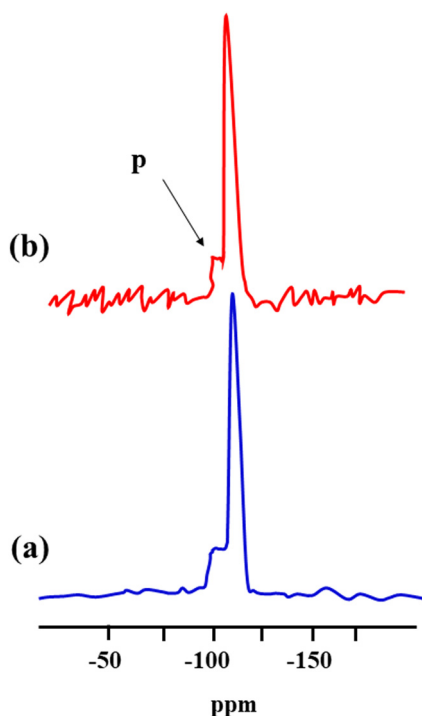
Figure 4: (a) ^{29}Si NMAS NMR spectrum of calcined Ga-Silicate-1. (b) CP ^{1}H ^{29}Si NMAS NMR spectrum of calcined Ga-Silicate-1.

Figure 4 reveals the ^{29}Si MAS NMR for the calcined Ga-Silicate-1 sample (Figure 4a). The large sharp peak was previously assigned to the Si(OSi)$_4$ unit. As for the signal designated as peak (p) in Figure 4b, it can be seen that there is no enhancement of this peak (p) in the CP MAS NMR when compared to the same peak in the ^{29}Si MAS NMR (Figure 4a), which has been attributed previously to Si(OSi)$_3$(OGa). There are also no chemical shift differences for peak (p) between ^{29}Si and ^{1}H-^{29}Si MAS NMR. The differences in chemical shift always occur when there is a ^{29}Si nucleus with directly bonded hydroxyl groups. Consequently, peak (p) is not due to the hydroxyl nests associated with the silicon atoms in the framework. It can therefore be assumed that a proportion of gallium is incorporated into the frame of pentasil. This result may be an indication that gallium has been substituted isomorphically in the zeolitic framework but not a certainty. Thus, the peak at –102 ppm in the ^{29}Si MAS NMR spectrum of Ga-Silicate-1 can be attributed to Si (1Ga) units.

3.2 Catalyst testing

The reaction of PO with CO$_2$ over Ga-Silicate-1 in the presence of TEABr as a co-catalyst was carried out in the
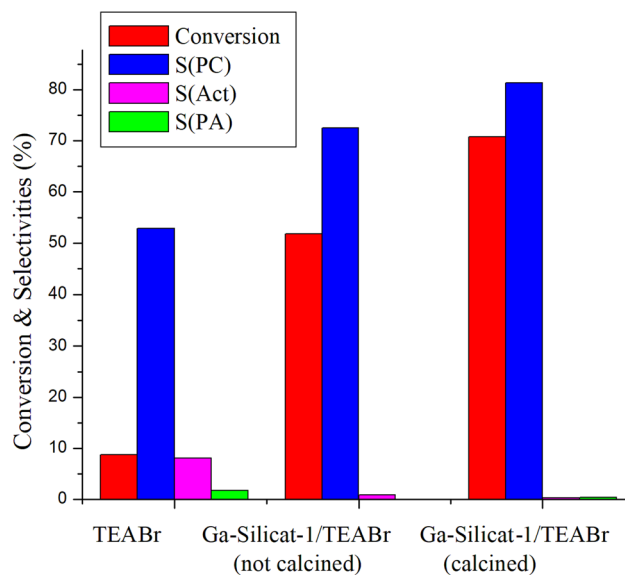

Figure 5: Conversion and product selectivities obtained over the co-catalyst alone (TEABr), as-synthesized Ga-Silicate-1/TEABr, and calcined Ga-Silicate-1/TEABr. Reaction conditions: R_t = 6 h, R_T = 75°C, $P(CO_2)$ = 0.55 MPa, 0.1 g of catalyst, and 0.1 g of co-catalyst.

liquid phase under mild conditions. Analysis by means of GC MS showed that the reaction (Scheme 1) led to PC as the major product, whereas acetone and propanal were obtained as minor products.

3.2.1 Role of TEABr

To determine the role of TEABr in PC synthesis, the following tests were performed: tests of TEABr (alone), as-synthesized Ga-Silicate-1 (alone and in the presence of TEABr), and Ga-Silicate-1 calcined at 350°C (alone and in the presence of TEABr). The results obtained showed that both the as-synthesized and calcined Ga-Silicate-1 did not give conversion values detectable in the gas chromatograph. In contrast, TEABr and as-synthesized Ga-Silicate-1 and calcined Ga-Silicate-1 in the presence of TEABr led to the formation of PC. The results are reported in Figure 5. Since these results showed that the reaction catalyzed by Ga-Silicate-1 in the presence of TEABr gave good conversion and good selectivity, it was decided to conduct the synthesis of PC by using Ga-Silicate-1 as the catalyst and TEABr as the co-catalyst.

3.2.2 Effect of calcination temperature

The effect of the calcination temperature was studied in the temperature range of 350–550°C. The results obtained
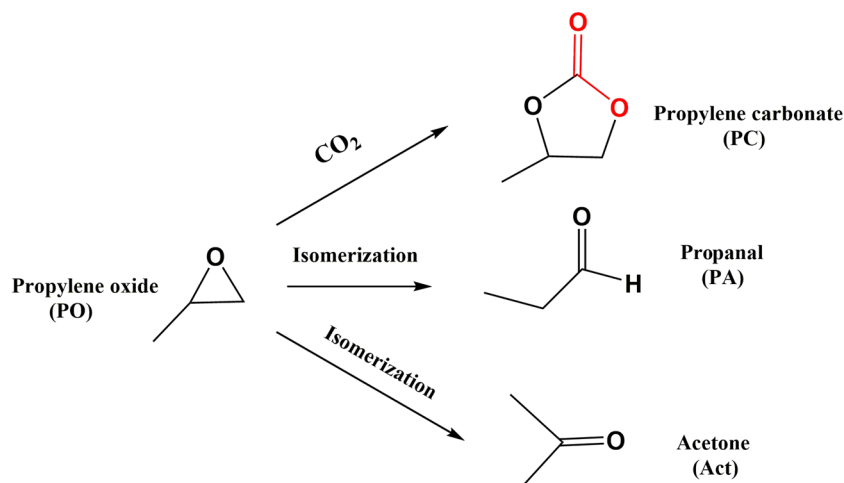
Scheme 1: Main products obtained in the reaction of CO_2 with PO over the Ga-Silicate-1/TEABr catalyst system.

(Figure 6) showed that when the temperature was increased from 500°C to 550°C, both the conversion and selectivity to PC dropped from 63.7% to 20.6% and from 77.6% to 58.9%. Contrary to the conversion and PC selectivity, the surface area increased slightly when the temperature increases from 350°C to 500°C and then increased rapidly beyond 500°C. In fact, when the temperature increased from 500°C to 550°C, the surface
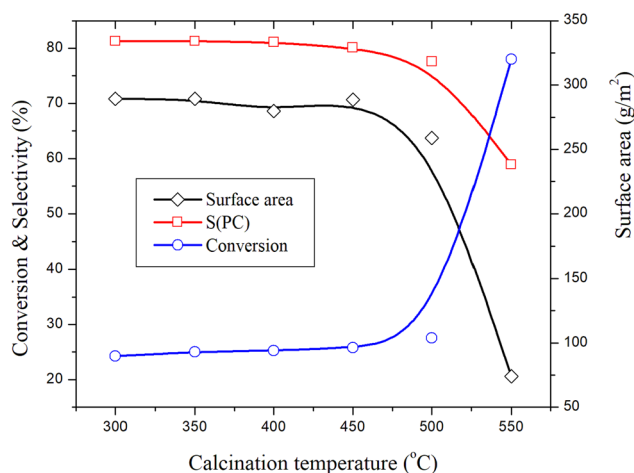

Figure 6: Effect of the calcination temperature on the surface area, conversion, and selectivity for PC. Reaction conditions: R_t = 6 h, R_T = 75°C, $P(CO_2)$ = 0.55 MPa, 0.3 g of catalyst, and 0.1 g of co-catalyst.

area increased from 96.1 to 103.8 m^2/g. This significant increase of the surface area is due to the removal of the gallium from the framework of the zeolite (Table 2). This result is in agreement with those reported in the literature [25]. Indeed, it has been reported that the degree of degalliation depends on the Si/Ga ratio of the as-synthesized material. This has been explained by the fact that the large amount of water released by the as-synthesized material during the hydrothermal treatment accentuates the elimination of trivalent elements from the frame during calcination. The degalliation caused by hydrothermal treatments of samples [Ga]-ZSM-5 has also been reported by other authors [45,46]. The loss of gallium led to a considerable decrease of the conversion and PC selectivity. This result indicated clearly that the presence of gallium enhances the reaction of PO with CO_2. So the catalyst calcined at 350°C was used for further investigations.

3.2.3 Effect of reaction temperature

The effect of reaction temperature was investigated in the temperature range from 60°C to 75°C. The experiments were carried out under a pressure of CO_2 equal to 0.55 MPa for 6 h over the catalyst calcined at 350°C. The

Table 2: Composition obtained by wet chemical analysis of the as-synthesized Ga-Silicate-1 and that calcined at 550°C

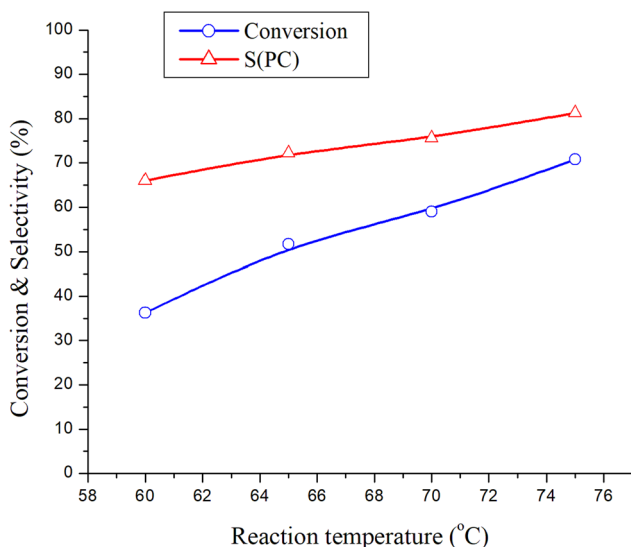| Sample phase	SiO_2/Ga_2O_3	Si/Ga	SiO_2/Al_2O_3	Si/Al	Al/Na	Ga/Na
As-synthesized	83	41.5	1,632	816	0.01	1.22
Calcined at 550°C	90	45.0	1,209	604.5	0.04	0.44

Figure 7: Effect of reaction temperature on the conversion and selectivity of PC. Reaction conditions: R_t = 6 h, $P(CO_2)$ = 0.55 MPa, 0.3 g of Ga-Silicate-1 calcined at 350°C, and 0.1 g of co-catalyst.

Figure 8: Arrhenius plot for the reaction of PO with CO_2 over Ga-Silicate-1 calcined at 350°C. Reaction conditions: R_t = 6 h, $P(CO_2)$ = 0.55 MPa, 0.3 g of Ga-Silicate-1 calcined at 350°C, and 0.1 g of co-catalyst.

results obtained (Figure 7) showed that temperature has a strong effect on the conversion and selectivities. In fact, the conversion increased sharply whereas the selectivity for PC increased slowly when the temperature was increased, and in this range of temperatures, the conversion increased from 36.3% to 70.8 % and the selectivity for PC increased from 66% to 81.3%. This very slight increase in the selectivity for PC might be caused by the increase of secondary reactions such as isomerization to acetone, as well as hydrolysis to diol, favored at high temperatures [47,48]. In order to evaluate the efficiency of the Ga-Silicate-1 catalyst in cyclic carbonate synthesis, the activation energy (E_a) was evaluated. E_a was determined from the Arrhenius equation by plotting $\ln[Y(PC)]$ (yield of PC) obtained at different temperatures against $1/T$, and the result is shown in Figure 8. The Arrhenius equation was found to be quite obeyed, and the calculated activation energy (E_a = 20.7 kJ/mol) was much lower than those reported in the literature with various catalyst systems [49–53]. The smallest E_a value of the Ga-Silicate-1 catalyst demonstrates its efficacy to accelerate the reaction rate.

3.2.4 Effect of reaction time

The dependence of the conversion and PC selectivity on reaction time at 75°C and a CO_2 pressure of 0.55 MPa is shown in Figure 9. The results indicate that both the conversion and selectivity to PC increase gradually when the reaction time was increased from 2 to 6 h. A PO
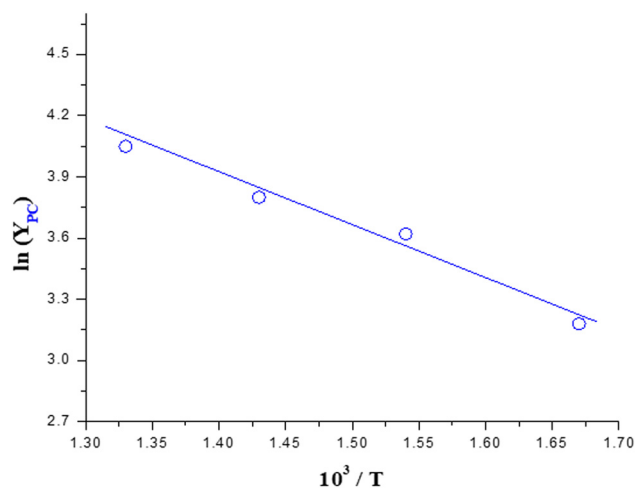
conversion of 70.8% and a selectivity for PC of 81.3% were obtained within 6 h. After 6 h of reaction, no significant change in both the conversion rate and the selectivity for PC was observed. This result indicates that the equilibrium of the reaction was reached.

3.2.5 Effect of CO_2 pressure

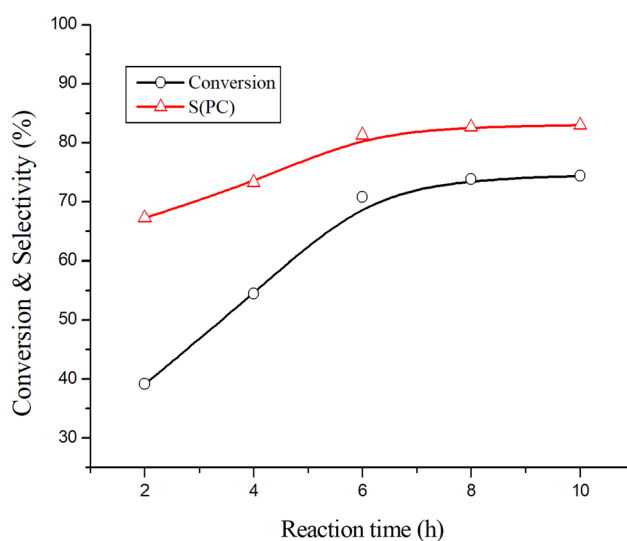The effect of CO_2 pressure was investigated, and the results are depicted in Figure 10. It can be seen from the

Figure 9: Effect of reaction time on the conversion and PC selectivity. Reaction conditions: R_T = 75°C, $P(CO_2)$ = 0.55 MPa, 0.3 g of Ga-Silicate-1 calcined at 350°C, and 0.1 g of co-catalyst.
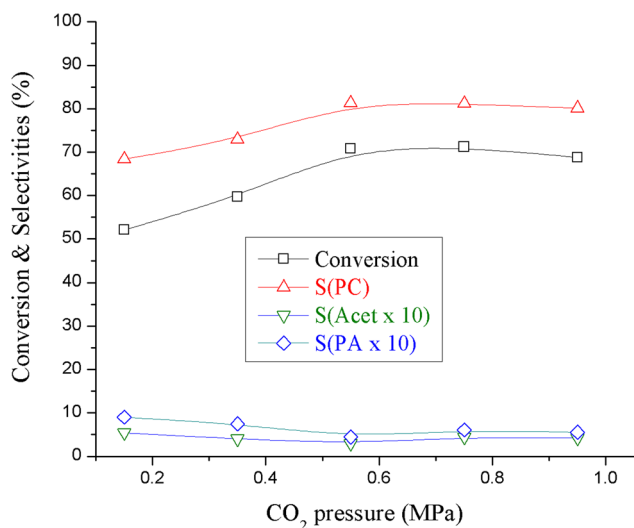
Figure 10: Effect of CO$_2$ pressure on conversion and PO selectivity. Reaction conditions: R_t = 6 h, R_T = 75°C, 0.3 g of Ga-Silicate-1 calcined at 350°C, and 0.1 g of co-catalyst.

figure that increasing the CO$_2$ pressure increased the conversion until it reached a maximum value of 70.8% at a pressure of 0.55 MPa. A further increase of CO$_2$ pressure decreased slightly both the conversion and PC selectivity. This can be explained by the effect of CO$_2$ pressure on the concentrations of CO$_2$ and PO in the two phases of the reaction medium [54]. The top phase is the CO$_2$-rich phase, and the bottom phase is the PO-rich phase. Since the reaction occurs in the liquid phase because of the presence of the catalyst in this phase, the conversion increased when the concentration of CO$_2$ increased in the bottom phase at low pressure, and it decreased when the concentration of PO decreased in the bottom phase at high pressure (>0.95 MPa). So, 0.55 MPa is the suitable pressure. The PC selectivity reaches a value of 81.3%. Based on the results obtained in this work, we can conclude that the appropriate reaction conditions for the synthesis of PC from PO and
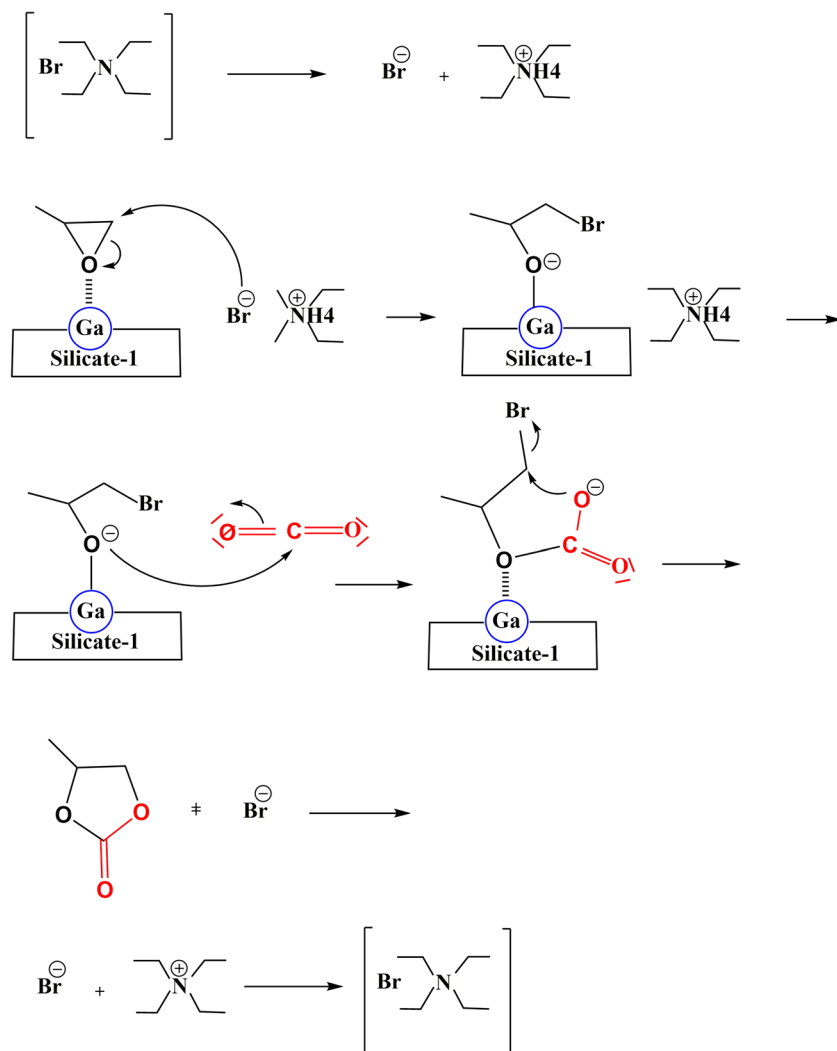
Scheme 2: Suggested mechanism for the synthesis of PC from PO and CO$_2$. Reaction catalyzed by the Ga-Silicate-1/TEABr catalyst system.

CO_2 are to operate at 75°C for 6 h under a pressure of CO_2 equal to 0.55 MPa. Under these conditions, PC was obtained with a yield of 57.6%. For comparison, a yield of 85% over ZnHZSM-5 zeolites prepared by an impregnation method was obtained [23]. ZnHZSM-5 was tested at 120°C, 1 MPa, and 8 h in the presence of tetra-*n*-propylammonium bromide as the co-catalyst. The yields obtained over FeHZSM-5 Fe, CoHZSM-5, and NiHZSM-5 were 35%, 53%, and 33%, respectively. A titanium-silicalite zeolite prepared by using polydiallyldimethylammonium chloride as the template was also tested for the cycloaddition of CO_2 to PO. The zeolite was not calcined in order to use the ammonium for activating the reaction. The conversion of PO obtained under 1.6 MPa at 120°C for 6 h when acetonitrile is used as a solvent reached 78.3% [24].

3.3 Proposed reaction mechanism

The proposed reaction mechanism for the synthesis of PC from PO and CO_2 catalyzed by the Ga-Silicate-1/TEABr catalyst system is illustrated in Scheme 2. First, the epoxidized oxygen is activated by the metal center of Lewis acid (Ga (II)) then, the bromide ion of the TEABr co-catalyst attacks the less hindered carbon atom, allowing the opening of the PO ring and leading to the formation of an alkoxy bromide intermediate. Then, the oxygen recovering its doublet shared with the gallium metal attacks the carbon of CO_2 to form a carboxylate anion, which in turn attacks the carbon atom of PO, thus allowing the release of the bromide ion and resulting in the cycloaddition.

4 Conclusion

Ga-Silicate-1 calcined at different temperatures was tested as a catalyst for the synthesis of PC from CO_2 and PO under mild conditions.

Increasing the calcination temperature from 500°C to 550°C increased the surface area (due to the removal of gallium oxide) but decreased the conversion. This result clearly indicates that the conversion depends on gallium content rather than surface area.

The low E_a value of the Ga-Silicate-1 catalyst compared to various catalytic systems demonstrates its effectiveness in catalyzing the coupling reaction of PO and CO_2. The production of PC depends on the CO_2

pressure range. High pressures decrease the conversion owing to the decrease of the amount of PO in the bottom phase containing the catalyst

The optimal conditions for a high production of PC are to carry out the reaction at 75°C under a CO_2 pressure equal to 0.55 MPa on a sample calcined at 350°C.

References

[1]   Clements JH. Reactive applications of cyclic alkylene carbonates. Ind Eng Chem Res. 2003;42(4):663–74.

[2]   Shaikh A-AG, Sivaram S. Organic carbonates. Chem Rev. 1996;96(3):951–76.

[3]   Schaffner B, Schaffner F, Verevkin SP, Borner A. Organic carbonates as solvents in synthesis and catalysis. Chem Rev. 2010;110(8):4554–81.

[4]   Ju H-Y, Manju M-D, Kim K-H, Park S-W, Park D-W. Catalytic performance of quaternary ammonium salts in the reaction of butyl glycidyl ether and carbon dioxide. J Ind Eng Chem. 2008;14(2):157–60.

[5]   Zhao Y, Tian J-S, Qi X-H, Han Z-N, Zhuang Y-Y, He L-N. Quaternary ammonium salt-functionalized chitosan: an easily recyclable catalyst for efficient synthesis of cyclic carbonates from epoxides and carbon dioxide. J Mol Catal A. 2007;271(1–2):284–9.

[6]   Sun D, Zhai H. Polyoxometalate as co-catalyst of tetrabutylammonium bromide in polyethylene glycol (PEG) for coupling reaction of CO_2 and propylene oxide or ethylene oxide. Catal Commun. 2007;8(7):1027–30.

[7]   Peppel W. Preparation and properties of the alkylene carbonates. Ind Eng Chem. 1958;50(5):767–70.

[8]   Wang S, Xi C. Recent advances in nucleophile-triggered CO_2-incorporated cyclization leading to heterocycles. Chem Soc Rev. 2019;48(1):382–404.

[9]   Daghagheleh M, Vali M, Rahmani Z, Sarhandi S, Vessally E. A review on the CO_2 incorporation reactions using arynes. Chem Rev Lett. 2018;1(1):23–30.

[10]   Ema T, Fukuhara K, Sakai T, Ohbo M, Bai F-Q, Hasegawa J-Y. Quaternary ammonium hydroxide as a metal-free and halogen-free catalyst for the synthesis of cyclic carbonates from epoxides and carbon dioxide. Catal Sci Technol. 2015;5(4):2314–21.

[11]   Yano T, Matsui H, Koike T, Ishiguro H, Fujihara H, Yoshihara M, et al. Magnesium oxide-catalysed reaction of carbon dioxide with anepoxide with retention of stereochemistry. Chem Commun. 1997;12:1129–30.

[12]   D'Elia V, Dong H, Rossini AJ, Widdifield CM, Vummaleti SV, Minenkov Y, et al. Cooperative effect of monopodal silica-supported niobium complex pairs enhancing catalytic cyclic carbonate production. J Am Chem Soc. 2015;137(24):7728–39.

[13] Martín C, Fiorani G, Kleij AW. Recent advances in the catalytic preparation of cyclic organic carbonates. ACS Catal. 2015;5(2):1353–70.

[14] Zhou Z, He C, Xiu J, Yang L, Duan C. Metal – organic polymers containing discrete single-walled nanotube as a heterogeneous catalyst for the cycloaddition of carbon dioxide to epoxides. J Am Chem Soc. 2015;137(48):15066–9.

[15] Song Y, Cheng C, Jing H. Aza-crown ether complex cation ionic liquids: preparation and applications in organic reactions. Chem Eur J. 2014;20(40):12894–900.

[16] Al Kahtani A, Abduh NA, Aouissi A. Synergistic effect between CO₂ and H₂O₂ on ethylbenzene oxidation catalyzed by carbon supported heteropolyanion catalysts. Green Proc Synth. 2019;8(1):85–92.

[17] North M, Pasquale R, Young C. Synthesis of cyclic carbonates from epoxides and CO₂. Green Chem. 2010;12(9):1514–39.

[18] Férey G, Mellot-Draznieks C, Serre C, Millange F, Dutour J, Surblé S, et al. A chromium terephthalate-based solid with unusually large pore volumes and surface area. Science. 2005;309(5743):2040–2.

[19] Widiastuti N, Thalib F, Prasetyoko D, Fansuri H. Ukuran partikel dan konformasi kristal zeolit – a hasil sintesis dengan penambahan tetrapropilammonium hidroksida (TPAOH). Reaktor 15(2):132–8.

[20] Wardani AR, Widiastuti N. Synthesis of Zeolite-X supported on glasswool for CO₂ capture material: variation of immersion time and NaOH concentration at glasswool activation. Indonesian J Chem. 2016;16(1):1–7.

[21] Fleischer M, Hanrieder W, Meixner H. Stability of semiconducting gallium oxide thin films. Thin Solid Films. 1990;190(1):93–102.

[22] Li L, Fan S, Mu X, Mi Z, Li C-J. Photoinduced conversion of methane into benzene over GaN nanowires. J Am Chem Soc. 2014;136(22):7793–6.

[23] Zhao QN, Song QW, Liu P, Zhang QX, Gao JH, Zhang K. Catalytic conversion of CO₂ to cyclic carbonates through multifunctional zinc-modified ZSM-5 zeolite. Chin J Chem. 2018;36(3):187–93.

[24] Liu D, Li G, Liu J, Wei Y, Guo H. Mesoporous titanium-silicalite zeolite containing organic templates as a bifunctional catalyst for cycloaddition of CO₂ and epoxides. ACS Appl Mater Interfaces. 2018;10(26):22119–29.

[25] Fricke R, Kosslick H, Lischke G, Richter M. Incorporation of gallium into zeolites: syntheses, properties and catalytic application. Chem Rev. 2000;100(6):2303–406.

[26] Mowry J, Anderson R, Johnson J. Process makes aromatics from LPG. Oil Gas J. 1985;83(48):128–31.

[27] Phatanasri S, Praserthdam P, Sripusitto A. Aromatization of light paraffins over Ga-containing MFI-type catalyst. Korean J Chem Eng. 2000;17(4):409–13.

[28] Han J, Jiang G, Han S, Liu J, Zhang Y, Liu Y, et al. The fabrication of Ga₂O₃/ZSM-5 hollow fibers for efficient catalytic conversion of n-butane into light olefins and aromatics. Catalysts. 2016;6(1):13.

[29] Nakai M, Miyake K, Inoue R, Ono K, Al Jabri H, Hirota Y, et al. Dehydrogenation of propane over high silica* BEA type gallosilicate (Ga-Beta). Catal Sci Technol. 2019;9(22):6234–9.

[30] Hwang YK, Jin T, Kim JM, Kwon Y-U, Park S-E, Chang J-S. Microwave synthesis of metallosilicate zeolites with fibrous morphology. J Nanosci Nanotechnol. 2006;6(6):1786–91.

[31] Xue T, Wang YM, He M-Y. Facile synthesis of nano-sized NH4-ZSM-5 zeolites. Microporous Mesoporous Mater. 2012;156:29–35.

[32] Chevella D, Macharla AK, Banothu R, Gajula KS, Amrutham V, Boosa M, et al. Synthesis of non-symmetrical alkyl carbonates from alcohols and DMC over the nanocrystalline ZSM-5 zeolite. Green Chem. 2019;21(11):2938–45.

[33] Cheng Y, Wang L-J, Li J-S, Yang Y-C, Sun X-Y. Preparation and characterization of nanosized ZSM-5 zeolites in the absence of organic template. Mater Lett. 2005;59(27):3427–30.

[34] Al-Dughaither AS, de Lasa H. HZSM-5 zeolites with different SiO₂/Al₂O₃ ratios. Characterization and NH₃ desorption kinetics. Ind Eng Chem Res. 2014;53(40):15303–16.

[35] Treacy MM, Higgins JB. Collection of simulated XRD powder patterns for zeolites fifth (5th) revised edition. Amsterdam: Elsevier Science; 2007.

[36] Nakasaka Y, Tago T, Masuda T. Synthesis of light olefins from oxygenated organic compounds over metallosilicates with MFI and MTW-type zeolite structures. J Jpn Pet Inst. 2017;60(6):277–87.

[37] Awate S, Joshi P, Shiralkar V, Kotasthane A. Synthesis and characterization of gallosilicate pentasil (MFI) framework zeolites. J Incl Phenom Mol Recognit Chem. 1992;13(3):207–18.

[38] Hu P, Iyoki K, Yamada H, Yanaba Y, Ohara K, Katada N, et al. Synthesis and characterization of MFI-type zincosilicate zeolites with high zinc content using mechanochemically treated Si–Zn oxide composite. Microporous Mesoporous Mater. 2019;288:109594.

[39] Koike N, Iyoki K, Keoh SH, Chaikittisilp W, Okubo T. Synthesis of new microporous zincosilicates with CHA zeolite topology as efficient platforms for ion-exchange of divalent cations. Chem A Eur J. 2018;24(4):808–12.

[40] Vieira LH, Carvalho KT, Urquieta-González EA, Pulcinelli SH, Santilli CV, Martins L. Effects of crystal size, acidity, and synthesis procedure on the catalytic performance of gallium and aluminum MFI zeolites in glycerol dehydration. J Mol Catal A Chem. 2016;422:148–57.

[41] Khodakov AY, Kustov L, Bondarenko T, Dergachev A, Kazansky V, Minachev KM, et al. Investigation of the different states of gallium in crystalline gallosilicates with pentasil structure and their role in propane aromatization. Zeolites. 1990;10(6):603–7.

[42] Jacob N, Joshi P, Shaikh A, Shiralkar V. Crystallization of gallium analog of zeolite Nu-23/ferrierite. Zeolites. 1993;13(6):430–4.

[43] Xin M, Xing E, Gao X, Wang Y, Ouyang Y, Xu G, et al. Ga substitution during modification of ZSM-5 and its influences on catalytic aromatization performance. Ind Eng Chem Res. 2019;58(17):6970–81.

[44] Murakami Y, Iijima A, Ward JW. New developments in zeolite science and technology. Amsterdam: Elsevier Science; 1986.

[45] Bayense CR, van Hooff JH, Kentgens AP, de Haan JW, van de Ven LJ. The removal of gallium from the lattice of MFI-galosilicates as studied by 71 Ga mas-nmr spectroscopy. J Chem Soc Chem Commun. 1989;17:1292–3.

[46] Bayense CR, Kentgens AP, De Haan JW, Van de Ven LJ, Van Hooff JH. Determination of gallium in H (Ga) ZSM5 zeolites by gallium-71 MAS NMR spectroscopy. J Phys Chem. 1992;96(2):775–82.

[47] Sun J, Wang J, Cheng W, Zhang J, Li X, Zhang S, et al. Chitosan functionalized ionic liquid as a recyclable biopolymer-supported catalyst for cycloaddition of CO_2. Green Chem. 2012;14(3):654–60.

[48] Shi T-Y, Wang J-Q, Sun J, Wang M-H, Cheng W-G, Zhang S-J. Efficient fixation of CO_2 into cyclic carbonates catalyzed by hydroxyl-functionalized poly (ionic liquids). RSC Adv. 2013;3(11):3726–32.

[49] Kim D, Na K. Organic-inorganic multifunctional hybrid catalyst giving catalytic synergies in cooperative coupling between CO_2 and propylene oxide to propylene carbonate. J CO_2 Utilization. 2018;27:129–36.

[50] Jiang X, Gou F, Jing H. Alternating copolymerization of CO_2 and propylene oxide catalyzed by C_{2v}-porphyrin cobalt: selectivity control and a kinetic study. J Catal. 2014;313:159–67.

[51] Fu X, Jing H. Quaternary onium modified SalenCoXY catalysts for alternating copolymerization of CO_2 and propylene oxide: a kinetic study. J Catal. 2015;329:317–24.

[52] Darensbourg DJ, Fitch SB. An exploration of the coupling reactions of epoxides and carbon dioxide catalyzed by tetramethyltetraazaannulene chromium (III) derivatives: formation of copolymers versus cyclic carbonates. Inorg Chem. 2008;47(24):11868–78.

[53] Langanke J, Greiner L, Leitner W. Substrate dependent synergetic and antagonistic interaction of ammonium halide and polyoxometalate catalysts in the synthesis of cyclic carbonates from oleochemical epoxides and CO_2. Green Chem. 2013;15(5):1173–82.

[54] Xiong Y, Bai F, Cui Z, Guo N, Wang R. Cycloaddition reaction of carbon dioxide to epoxides catalyzed by polymer-supported quaternary phosphonium salts. J Chem. 2013;2013:261378.